

# Fractional Order Sliding Mode Controller Modelling for Fractional Order SEPIC Converter

Sena Alemu<sup>1\*</sup>,<sup>2</sup>Prashanth Alluvada,<sup>3</sup>Amruth Ramesh Thelkar,<sup>4</sup>N Samanvita<sup>5</sup>Tolcha Lemma,<sup>6</sup>Kifle Godana  
<sup>1,2,5,6</sup> Faculty of Electrical & Computer Engineering, Jimma Institute of Technology,  
Jimma University, Ethiopia.

<sup>3</sup>Electrical & Electronics Engineering Department, Nitte Meenakshi Institute of Technology  
Bangalore, Visvesvaraya Technological University ,Karnataka,India, & Faculty of Electrical & Computer  
Engineering, Jimma Institute of Technology,Jimma University, Ethiopia.

<sup>4</sup>Electrical & Electronics Engineering Department, Nitte Meenakshi Institute of Technology  
Bangalore, Visvesvaraya Technological University ,Karnataka,India

Corresponding Author Email Id: [amruth.ramesh@nmit.ac.in](mailto:amruth.ramesh@nmit.ac.in) , [amruth.ramesh@ju.edu.et](mailto:amruth.ramesh@ju.edu.et)

## Abstract

DC/DC converters are power electronic devices that utilize passive components such as resistors, capacitors, and inductors, along with transistors to control the system through a duty cycle. Traditionally modeled and controlled using integer-order calculus, these converters are now increasingly examined through the lens of fractional calculus, which introduces a fractional order for the controller, adding a new modulating variable beyond just the duty cycle. However, if only the controller operates in a fractional manner while the plant remains integer-order, the advantages of fractional calculus are limited, leading to challenges in flexibility, degree of freedom, and overall accuracy. To address these limitations, proposing an Indirect Sliding Mode Adaptive Fractional Order Controller (FOSMC) for Fractional Order Systems in Single-Ended Primary Inductor Converters (FOSEPIC). Utilizing the Caputo fractional derivative, mathematical model is developed to resolve the average state space equation of the DC/DC SEPIC converter. The Mittag-Leffler function, along with Lyapunov methods, is employed to analyze the system's dynamic stability. The performance of the proposed controller is assessed using the Integral Time Absolute Error (ITAE), yielding an ITAE of 0.09151, which is lower than that of the Fractional Order Model (0.1847) and the Integer Order Sliding Mode Controller (0.2532). Simulation results further demonstrate that the proposed strategy enhances efficiency to 98%. Overall, the FOSMC exhibits improved flexibility, a high degree of freedom, and superior accuracy, offering a fast transient response in controlling DC/DC converters.

Keywords: Fractional calculus, Single-Ended Primary Inductor Converters, Fractional order sliding mode control; Fractional order SEPIC converter.

## 1. Introduction

"Non-integer calculus," frequently referred to as "fractional calculus," includes not only integer orders but also generalized functional orders such as fractional, irrational, and complex orders. This broadens its scope, positioning it as a form of generalized calculus [1]. The historical roots of fractional calculus date back to 1695, when Leibniz proposed half-order derivatives in correspondence with L'Hospital. The ability of fractional calculus to model the dynamics of various natural phenomena provides more accurate descriptions than traditional integer-order dynamic systems with the advantage of a high degree of freedom, nonlocality, flexibility, nonuniformity, and memory effect. Due to these advantages, its applications span multiple fields, including control engineering, biology, biomedical engineering, financial markets, and signal processing. In electrical engineering, fractional calculus is increasingly

recognized for its utility in modeling electrical equipment, wireless power transmission systems, and studying chaotic behaviors in fractional-order dynamic systems[2][3]. Recent advancements have led to practical designs in areas such as electrode-electrolyte polarization, viscoelastic fluids, and power converters. However, conventional integer-order models often fail to adequately represent the behavior of inductors and capacitors and uniform definitions of orders of differentiation [4][5]. DC-DC converters have demonstrated that output voltage gain can be controlled only by the duty cycle while modeling using integer order calculus. The stability and differentiability characteristics of integer-order systems further enhance their appeal, as some non-differentiable functions. As well as integer-order models (IOM) can capture some characteristics, they often lack the necessary accuracy. These unique properties motivate ongoing research into the applications of fractional calculus across various physical and natural phenomena[6].

Recent studies have illustrated the effectiveness of fractional calculus in controller design and modeling different nonlinear dynamic systems, particularly DC-DC converters[7][8][11].

DC/DC (Direct Current to Direct Current) converters are power electronics devices composed of passive components like inductors, capacitors, resistors, and transistors functioning as switches. These converters are extensively used in various fields such as communications, industrial applications, and as power supplies for personal computers. Buck converters, boost converters, buck-boost converters, Cuk converters, and Single-Ended Primary Inductor Converter (SEPIC) converters are some of the most well-known DC/DC converters. Disturbances in most DC/DC converters arise from load variations, input voltage uncertainty, and electromagnetic interference generated from transistors, which complicate their control. Among these, the SEPIC converter is non-inverting, maintaining a positive output when the input is positive, and functions as both a step-up (BOOST) and step-down (BUCK) converter. It is particularly useful in applications requiring low ripple current at both input and output terminals and off-grid photovoltaic systems such as batteries and PV[9]. However, the SEPIC converter exhibits a non-linear variable structure with non-minimum phase characteristics, and instability, and is a time-varying system. Due to its non-minimum-phase nature (with zeros or poles at the origin), direct output voltage control is not feasible[10]. Consequently, to manage the output voltage of a SEPIC converter, the approach involves directly controlling the input current through the duty cycle and indirectly influencing the output voltage. Various controllers, such as PWM, PID, fuzzy logic controller, and sliding mode controls, are employed to regulate the SEPIC converter's operation[9].

A type of controller design known as a nonlinear variable structure (NVS) utilizes a nonlinear control rule based on a set of switching variable signals[1][11] [12]. Sliding mode control is closely related to NVS, as it can be used to design NVS controllers that provide stable control and smooth transitions between different control behaviors[13]. This approach can be applied to SEPIC converters to improve stability, adaptability, and efficiency. Given the intricate behaviors of the SEPIC converter, a sliding mode controller is selected among the possible options. The nonlinear behavior of the SEPIC converter[14], indicated by a specific characteristic, aligns with the requirements met by the sliding mode controller, making it an ideal choice. This control method allows the converter to operate in two modes: step-up (boost) when the reference voltage is greater than the input voltage, and step-down (buck) when the reference voltage is less than the input voltage, all with a single controller. Which give new circuit topologies based on these elements continue to emerge, although their characteristics remain an active area of research [15][16][11][17] and, enhance the analysis of their dynamic behavior[18][12].

Sliding Mode Control (SMC) is a highly effective strategy for Controlling uncertainties in both linear and nonlinear systems. Known for its rapid dynamics and excellent transient response, SMC offers robustness against external disturbances and parameter variations. The primary goal of SMC is to guide system states to a predefined manifold, called the sliding surface, and to maintain this state despite uncertainties [19][20]. The design of SMC consists of two phases: (i) the Reaching Phase and (ii) the Sliding Phase. In the Reaching Phase, system states are driven to the sliding manifold in finite time, but this phase can be sensitive to disturbances and parameter variations. To mitigate this sensitivity, various methods have been proposed to minimize or eliminate the reaching phase. During the Sliding Phase, the closed-loop system enters a sliding motion where robustness and order reduction become critical. In this phase, trajectories are less sensitive to disturbances and parameter variations, enhancing the robustness of SMC. However, it is important to note that robustness is not guaranteed during the Reaching Phase[21][22][23].

When traditional integer-order SMC methods are applied to fractional-order systems, they effectively reject disturbances but often suffer from chattering a significant drawback. The fundamental feature of SMC is that the state slides along the sliding surface. Conventional SMC typically employs a fixed, predefined sliding surface, which can lead to extended reaching times if the initial state is far from the surface, ultimately degrading control performance. Increasing the discontinuous control gain may shorten the reaching phase but can also exacerbate chattering issues [19][24][25].

Fractional calculus has shown promise in addressing the chattering problem and improving control performance. By incorporating fractional-order elements into SMC design, the chattering issue can be mitigated, and the response time of the closed-loop system can be enhanced. Fractional-order controllers provide additional design parameters, such as adjustable non-integer differentiator and integrator orders, allowing for the tuning of the fractional order to optimize dynamic response while preserving the advantages of conventional sliding mode control(SMC) [26][27][28][29][30].

Despite the demonstrated advantages of fractional calculus in various applications, its specific implementation in controlling DC-DC converters, particularly the SEPIC converter, remains underexplored. While existing studies have utilized fractional calculus in controller design, few have focused on its ability to manage the complex nonlinearities and non-minimum phase characteristics inherent in SEPIC converters. This research aims to fill this gap by demonstrating how an Indirect Sliding Mode Adaptive Fractional Order Controller (FOSMC) can effectively enhance the control performance and reliability of the SEPIC converter, ultimately contributing to more efficient power conversion systems.

## 2. Proposed Methods

In this study, the proposed a Fractional Order Sliding Mode Controller (FOSMC) designed specifically for a Fractional Order SEPIC Converter. The proposed method enhances traditional SMC by incorporating fractional calculus principles, which address the limitations of conventional integer-order controllers, particularly chattering and performance degradation during the reaching phase.

*I.Grunwald-Letnikov Fractional-Order Derivative:*The Grunwald-Letnikov fractional-order derivative is defined as:

$$D_{t\alpha}f(t) \equiv h^{-\alpha} \sum_{i=0}^{\infty} (-1)^i \binom{\alpha}{i} f(t - ih) \quad (1)$$

When the sign of  $\alpha$  is negative, this equation becomes a fractional-order integral[31][32].

*II. Riemann-Liouville (RL) Fractional-Order Integral:* Cauchy's formula for repeated integration reduces n-fold integration of a function  $f(t)$  to a single integral:

$$J_t^n f(t) = \int_0^t (t-x)^{n-1} f(x) dx \quad (2)$$

This can be generalized to a fractional-order integral:

$$J_t^n f(t) = \frac{1}{\Gamma(1+\alpha)} \int_0^t (t-x)^\alpha f(x) dx \quad (3)$$

where  $\Gamma(n)$  is the Euler's

The left Riemann-Liouville fractional-order derivative of a function  $f(t)$  is defined as:

$$J_t^\alpha f(t) = \frac{1}{\Gamma(n-\alpha)} \int_0^t (t-\tau)^{n-\alpha-1} f(\tau) d\tau \quad (4)$$

where:  $n=[\alpha]$  is the smallest integer greater than or equal to  $\alpha$ ,  $\Gamma$  is the gamma function,  $f(n)(\tau)$  is the n-th derivative of  $f$  is the lower limit of the integral. The right Riemann-Liouville derivative is:

$$D_t^\alpha f(t) = \frac{1}{\Gamma(n-\alpha)} \int_\alpha^t (t-\tau)^{n-\alpha-1} f(\tau) d\tau \quad (5)$$

Where  $b$  is the upper limit of the integral.

*III. Caputo Fractional Derivative:* The Caputo fractional-order derivative modifies the Riemann-Liouville definition to allow for broader applications: The left Caputo fractional-order derivative is given by:

$$D_t^\alpha f(t) = \frac{1}{\Gamma(n-\alpha)} \int_\alpha^t (t-\tau)^{n-\alpha-1} f(\tau) d\tau \quad (6)$$

Where  $n=[\alpha]$  is the smallest integer greater than or equal to  $\alpha$ ,  $\Gamma$  is the gamma function,  $f(n)(\tau)$  is the n-th derivative of  $f$ ,  $a$  is the lower limit of the integral. The right Caputo derivative is defined similarly:

$$D_t^\alpha f(t) = \frac{1}{\Gamma(n-\alpha)} \int_0^b (t-\tau)^{n-\alpha-1} f(\tau) d\tau \quad (7)$$

where  $b$  is the upper limit of the integral.

#### IV. Mittag-Leffler Function

The one-parameter Mittag-Leffler function is crucial for modeling physical processes using fractional calculus:

$$E_\alpha(z) = \sum_{k=0}^{\infty} \frac{z^k}{\Gamma(k+\alpha)} \quad (8)$$

### 2.1. Properties of GL, RL, and Caputo Fractional Order Derivatives

Essential characteristics of fractional-order operators consist of:

#### I. Semigroup and Commutative Property

$$J_t^\alpha J_t^\beta(t) = J_t^\beta J_t^\alpha(t) = J_t^{\alpha+\beta}(t) \quad (9)$$

#### II. Consistency Property:

$$\lim_{\alpha \rightarrow n} J_t^\alpha f(t) = J_t^n f(t) \quad (10)$$

#### III. Constant Property:



Figure 1: Block diagram for proposed FOSMC controller and FOSEPIC converter

### 2.3.SEPIC Converter Models

The conventional SEPIC converter is described by the following equations:

$$\begin{aligned} {}^C D_t^\alpha X_1 &= \frac{1}{l_1} v_{in} - \frac{1}{l_1} (1-u)(x_3 + x_4) \\ {}^C D_t^\alpha X_2 &= \frac{1}{l_2} x_3 u - \frac{1}{l_2} (1-u)x_4 \\ {}^C D_t^\alpha X_3 &= \frac{1}{c_1} (1-u)x_1 - \frac{1}{c_1} u x_2 \\ {}^C D_t^\alpha X_4 &= \frac{1}{c_2} (1-u)(x_1 + x_2) - \frac{g}{c_2} x_4 \end{aligned} \quad (12)$$

The fractional-order SEPIC converter system is defined as:

$$\begin{aligned} {}^C D_t^\alpha X_1 &= \frac{1}{l_1} v_{in} - \frac{1}{l_1} (1-u)(x_3 + x_4) \\ {}^C D_t^\alpha X_2 &= \frac{1}{l_2} x_3 u - \frac{1}{l_2} (1-u)x_4 \\ {}^C D_t^\alpha X_3 &= \frac{1}{c_1} (1-u)x_1 - \frac{1}{c_1} u x_2 \\ {}^C D_t^\alpha X_4 &= \frac{1}{c_2} (1-u)(x_1 + x_2) - \frac{g}{c_2} x_4 \end{aligned} \quad (13)$$

The output voltage is indirectly controlled by the input inductor current through the  $x_1$  state variable[33].

### 2.4.Sliding Mode Control

To achieve control, the sliding surface function is defined as:

$$s(t) = x_1 - x_r \quad (14)$$

where  $x_r$  denotes the reference for the  $x_1$  state variable. The inductor current reference can be generated using a proportional-integral (PI) controller without a compensation term:

$$x_r = -\lambda x_1 r - \varepsilon \int_0^t x_1 r dt \quad (15)$$

Here,  $\lambda$  and  $\varepsilon$  are the proportional and integral gains, respectively. The derivative can be expressed as:

$$D x_r = -\lambda D x_1 r - \varepsilon x_1 r \quad (16)$$

By applying the properties of fractional calculus, we can obtain:

$$D^\alpha D^{-\alpha} D x_1 r - \varepsilon x_1 r \quad (17)$$

### 2.5.Stability of the Sliding Dynamics

In a fractional differential system described by  $D_t^\alpha x(t) = f(t)$  where  $x=0$  is the equilibrium point, the function  $f(t)$  is assumed to be Lipschitz continuous. Under these conditions, the solutions of the system exhibit Mittag-Leffler stability. This means that if the initial state is close to the equilibrium, the solution will remain close over time, highlighting the system's ability to return to equilibrium despite perturbations. This behavior is particularly important in applications involving fractional dynamics, where traditional stability concepts may not apply. The reaching law is designed to ensure the stability of the closed-loop system:

$$D_t^\alpha s = -\gamma \text{sign}(s) - \rho s \quad (18)$$

where  $\rho > 0$  and  $\gamma > 0$ .

## 2.6. Control Law

Equating the fractional-order system dynamics with the reaching law leads to the control law:

$$D_t^\alpha x_1 + \lambda D_t^\alpha x_4 - \lambda D_t^\alpha x_4 d + \varepsilon D_t^{-\alpha} x_4 - \varepsilon D_t^{-\alpha} x_4 d - \gamma \text{sign}(s(t)) - \rho s(t) \quad (19)$$

From the SEPIC converter dynamics, the obtained equation:

$$D_t^\alpha x_1(t) = \alpha v_{in} - \alpha(1-u)(x_3 + x_4) \quad (20)$$

The control law can be expressed as:

$$u(t) = 1 - \frac{\alpha(x_3(t) + x_4(t))}{v_{in}} \quad (21)$$

This controller is applicable for both fractional-order and conventional SEPIC converters, depending on the value of  $\alpha$ . When  $0 < \alpha < 1$ , it functions as a fractional-order sliding mode controller, and when  $\alpha = 1$ , it behaves as a conventional sliding mode controller.

## 3. Results and Discussion

In this section, the presented simulation results of the modeled system to demonstrate the effectiveness of the proposed fractional-order sliding-mode control (SMC) scheme for the fractional-order nonlinear system. The theoretical considerations are validated through simulations conducted using the MATLAB/SIMULINK program. The performance of the proposed control method is evaluated based on its ability to regulate voltage under four varying conditions are Variable input voltage, Variable controller order, Variable system orders, Different load conditions.

The system and control parameters are employed here, with the simulation parameters detailed in Table 2.

**Table 2.** System and control parameters

No	Parameters	Value used
1	Input voltage( $v_{in}$ )	30V and 60V
2	Capacitors( $C_1, C_2$ )	330 $\mu$ F
3	Inductors( $L_1, L_2$ )	800 $\mu$ H
4	$V_{ref}$	48V
5	Prop/int gains( $\lambda, \epsilon$ )	25 and 10
6	load1 ( $R_{L1}$ )	50 $\Omega$
7	load2 ( $R_{L2}$ )	33.33 $\Omega$
8	input voltages	30V, 60V

### 3.1. Steady-State Performance

Figure 1 illustrates the steady-state results for the input voltage ( $v_{in}$ ), output voltage ( $v_{out}$ ), and inductor currents ( $i_{L1}$  and  $i_{L2}$ ) with a load resistance ( $R_L$ ) of 50 $\Omega$  in both buck and boost modes.

From Figures 1(a) and 1(c), it is evident that the output voltage is consistently maintained at 48V, indicating that the controller effectively regulates the output voltage to its reference value. Additionally, the inductor currents shown in Figures 1(b) and 1(d) demonstrate the performance in both boost and buck modes of operation. Overall, the converter, utilizing the proposed control method, successfully operates in both buck and boost modes, as depicted in Figure 1.

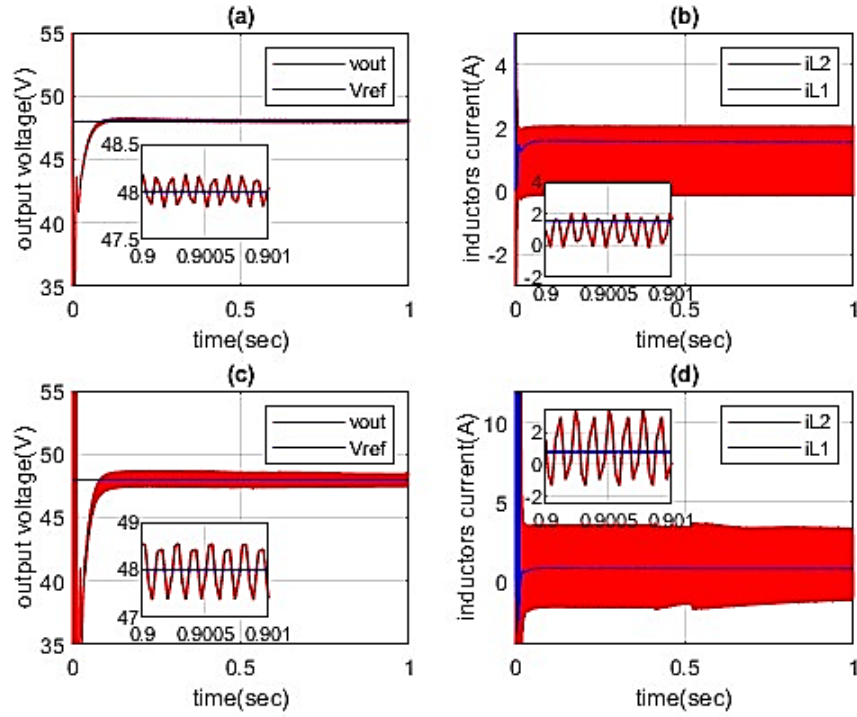


Figure 2. Steady-state performance of the FOSEPIC converter

Figure 2 presents the steady-state performance of the FOSEPIC converter, showcasing the output voltage and inductor currents in both boost and buck modes. Specifically, panel (a) illustrates the output voltage for the boost mode, while panel (b) displays the inductor current for the same mode. Panels (c) and (d) depict the output voltage and inductor current for the buck mode, respectively. The results indicate that the output voltage remains consistently regulated at 48V across both modes, demonstrating the effectiveness of the proposed control method in maintaining performance under varying operational conditions.



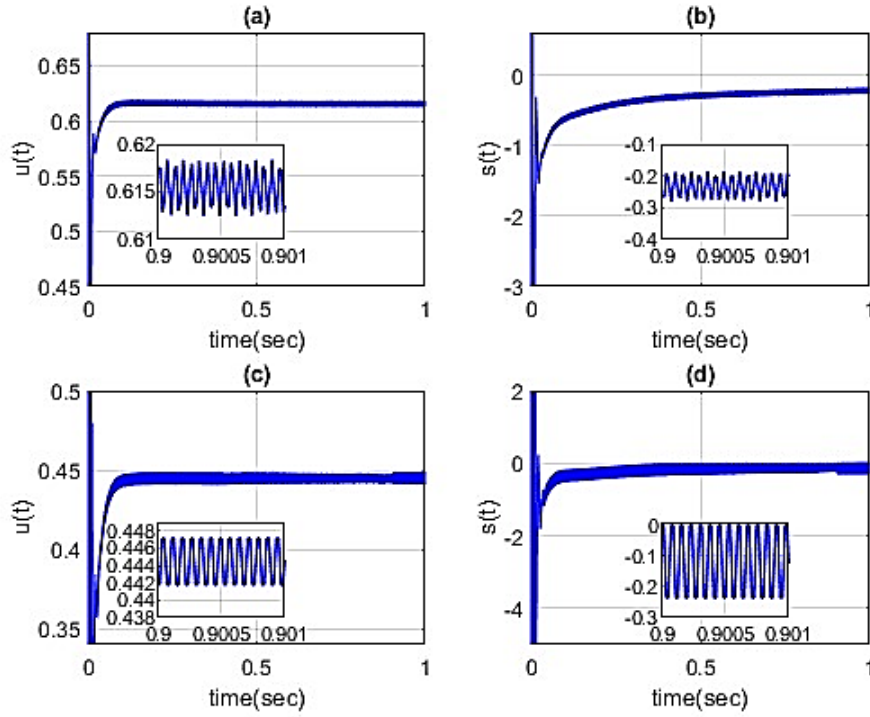


Figure 3. Fractional-order sliding mode controller (FOSMC) for the FOSEPIC converter

Figure 3 illustrates the fractional-order sliding mode controller (FOSMC) for the FOSEPIC converter, featuring the sliding surfaces and controller responses in both boost and buck modes. Panel (a) displays the FOSMC for the boost mode, while panel (b) shows the sliding surface for the boost mode. Similarly, panel (c) presents the FOSMC for the buck mode, and panel (d) depicts the sliding surface for the buck mode. This figure highlights the steady-state responses of the input voltage, output voltage, and inductor currents with a load resistance ( $RL$ ) of  $50\Omega$ .

### 3.2. Performance Under Input Voltage Variations

Figure 4 shows the dynamic responses of the inductor current ( $i_{L1}$ ) and output current ( $i_{out}$ ) following changes in the input voltage ( $v_n$ ), with a reference voltage  $V_{ref}$  of 48V and a load resistance of  $50\Omega$ . The results correspond to variations in input voltage from 60V to 30V and then back from 30V to 60V. Initially, the converter operates in buck mode at  $v_{in}=60V$ . When the input voltage decreases to 30V, the converter switches from buck mode to boost mode. Conversely, when the input voltage increases back to 60V, the operation shifts from boost mode to buck mode. During these transitions, the input current adjusts accordingly to ensure that the power delivered to the load remains constant, as illustrated in Figure 4 for both operating modes. Notably, the output voltage successfully maintains its reference level at 48V in both modes.

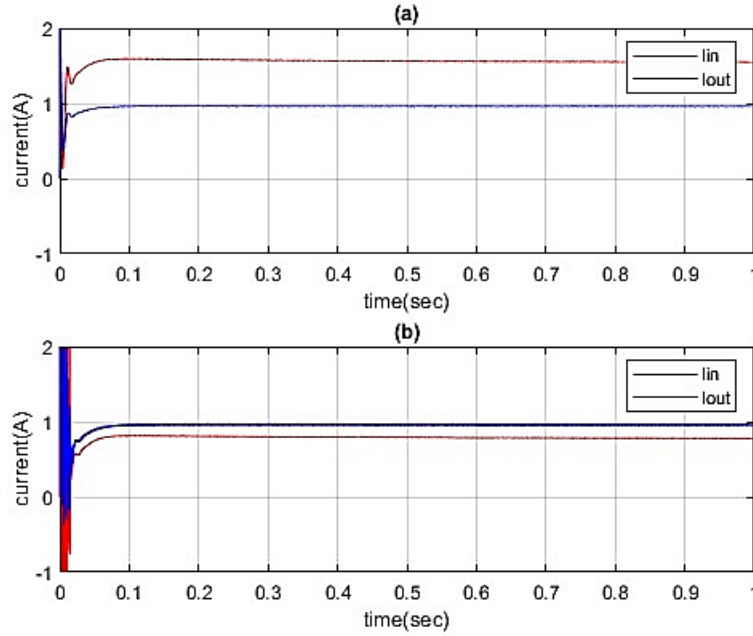


Figure 4. Input and Output Current for FOSEPIC Converter

Figure 4 presents the input and output currents for the FOSEPIC converter, with panel (a) depicting the currents during boost mode operation and panel (b) showing the currents during buck mode operation. It is evident that there are small, undesired ripples in the output current, likely resulting from noise disturbances within the system. Despite these ripples, the output voltage is consistently regulated at 48V in both operating modes. To maintain the load power amidst variations in input voltage, adjustments to the input current are necessary.

### 3.3.Performance Under Load Variations

The proposed control strategy's performance was further evaluated under load variations ranging from 50% to 70%. Figure 5 illustrates the dynamic responses of the output voltage in response to abrupt changes in load resistance, with a reference voltage ( $V_{ref}$ ) set at 48V. The load was switched from  $50\Omega$  to  $33.33\Omega$  and then back from  $33.33\Omega$  to  $50\Omega$ . Figures 6 and 7 display the dynamic responses during these load changes while the converter operates in both boost and buck modes, respectively. Notably, the output voltage remains largely unaffected by these load variations, demonstrating the controller's capability to regulate output voltage effectively. Although small overshoots and undershoots occur during the transient periods, the output voltage stabilizes quickly, confirming the robustness of the proposed control strategy under varying load conditions.

Figure 4. Input and Output Power for FOSEPIC Converter

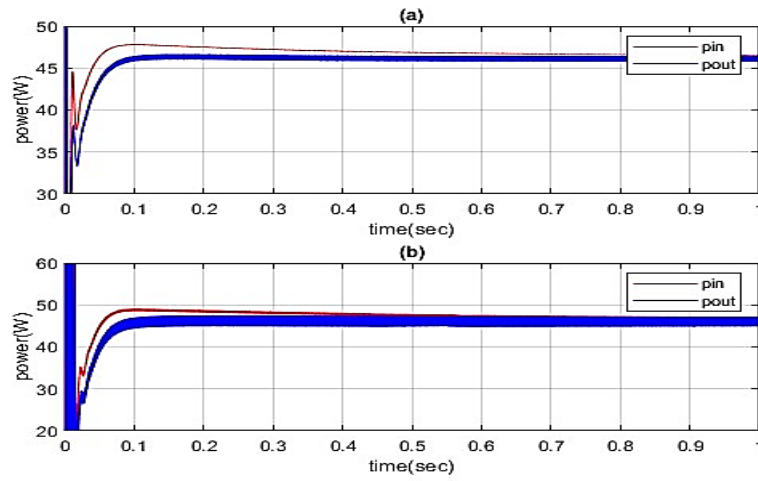


Figure 5. Input and Output Power for FOSEPIC Converter

Figure 5. Input and Output Power for FOSEPIC Converter (a) Output and Input Power for Boost Mode of Operation (b) Output and Input Power for Buck Mode of Operation.

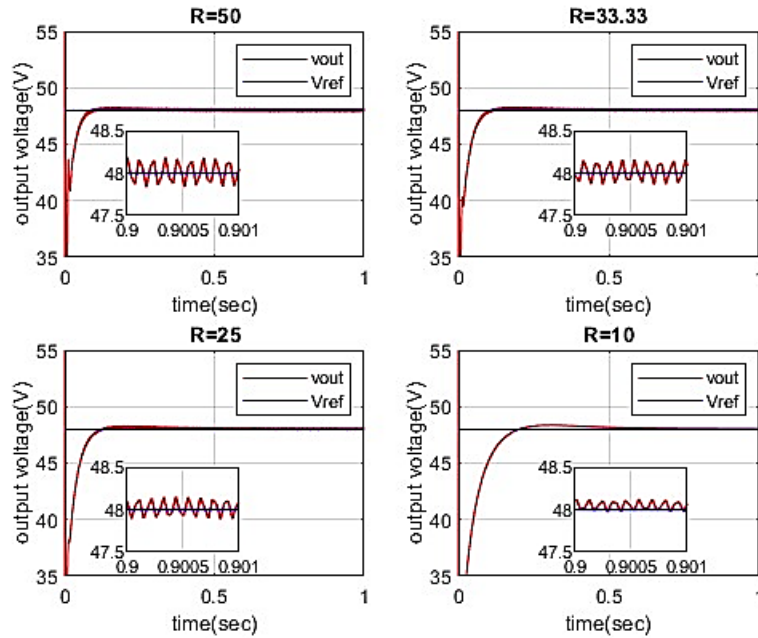


Figure 6. FOSEPIC Converter Under Load Variations for Boost Mode of Operation.

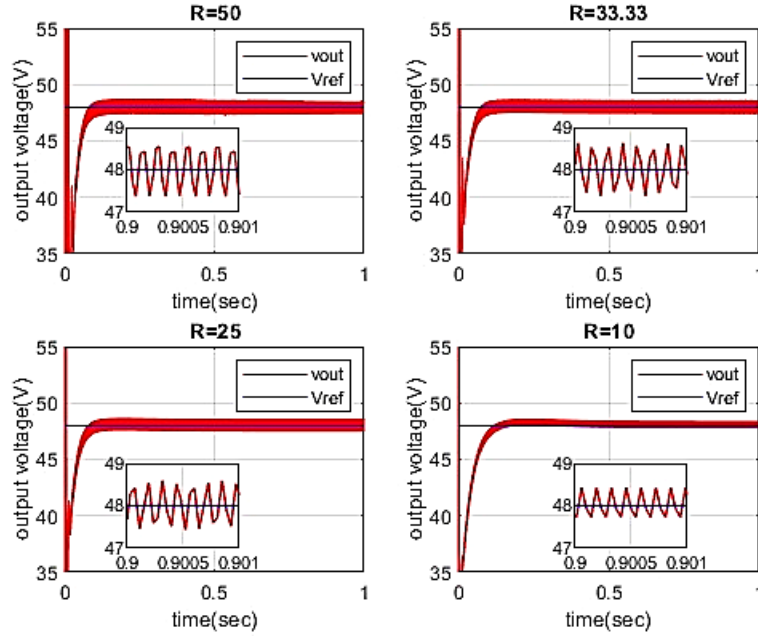


Figure 7. FOSEPIC Converter Under Load Variations for Buck Mode of Operation

During load variations, the two operating modes exhibit distinct behaviors regarding peak-to-peak output voltage. In boost mode, the converter demonstrates lower peak-to-peak values, whereas in buck mode, the peak-to-peak values are higher. Additionally, the response in buck mode shows increased peak-to-peak values for both output voltage and output current. Load variations in boost mode, with load resistance ranging from  $1\Omega$  to  $3k\Omega$ , and in buck mode, with a range of  $1\Omega$  to  $58\Omega$ , yield consistent results for the FOSEPIC converter with orders of (0.25, 0.35, 0.52, 0.65), effectively regulating around a reference voltage ( $V_{ref}$ ) of 48V.

### 3.4. Performance Under Variation of Plant Orders

In scenarios involving variations in plant orders, the fractional-order sliding mode controller (FOSMC) with an order of 0.35 successfully regulates the output voltage at  $V_{ref} = 48V$ , as demonstrated in Figure 8. This indicates the controller's robustness in maintaining voltage regulation across different system dynamics.

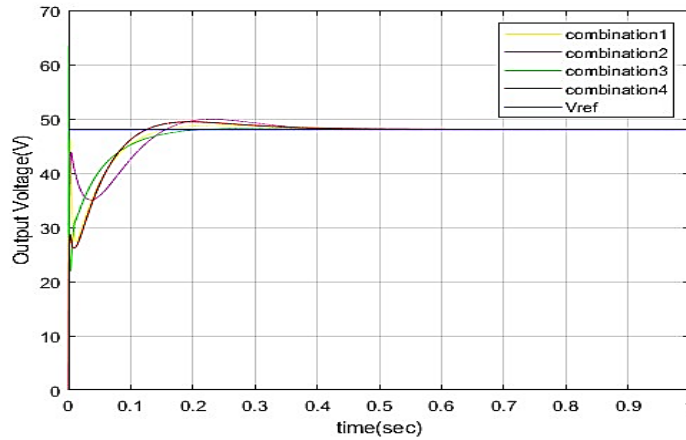


Figure 8. Output Voltage under Variation of FOSEPIC Orders

Figure 8 displays the output voltage variations corresponding to different combinations of FOSEPIC orders. Panel (a) illustrates the response for the combination of orders [Yellow] (0.6, 0.28, 0.4, 0.9), while panel (b) shows [Magenta] (0.9, 0.5, 0.4, 0.9). Panel (c) presents the output for [Green] (0.17, 0.25, 0.35, 0.69), and panel (d) displays the results for [Red] (0.75, 0.5, 0.2, 0.85). These results highlight how different order combinations affect the output voltage stability and regulation.

### 3.5. Comparison of FOSMC and SMC for FOSEPIC Converter

In the comparison of the fractional-order sliding mode controller (FOSMC) and the traditional sliding mode controller (SMC) for the FOSEPIC converter, as shown in figure 9 for boost mode, the FOSMC effectively minimizes oscillations that are prevalent in the SMC for the SEPIC configuration. This enhanced stability is similarly observed in the buck mode operation, indicating the superior performance of the FOSMC in maintaining output voltage regulation across varying operating conditions.

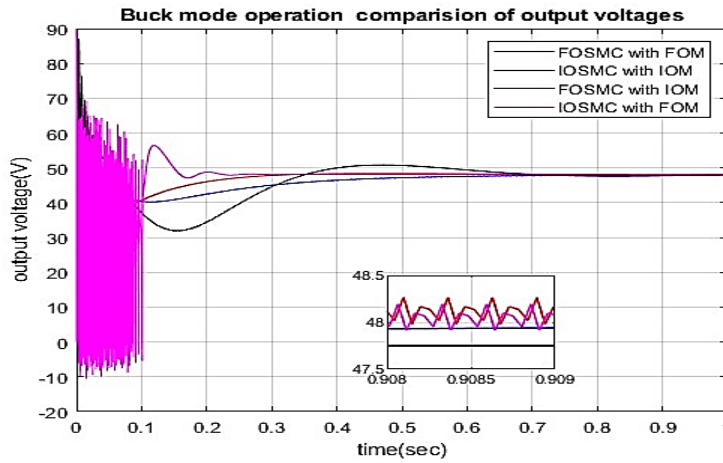


Figure 9. Comparison Output Voltage of SEPIC and FOSEPIC converter with FOMSC and IOSMC for Buck Mode Operation

Figure 9. Comparison Output Voltage of SEPIC and FOSEPIC converter with FOMSC and IOSMC for Buck Mode Operation (a)[Red] FOSMC with FOM (b)[Blue] IOSMC with IOM (c)[Black] FOSMC with IOM (d)[Magenta] IOSMC with FOM.

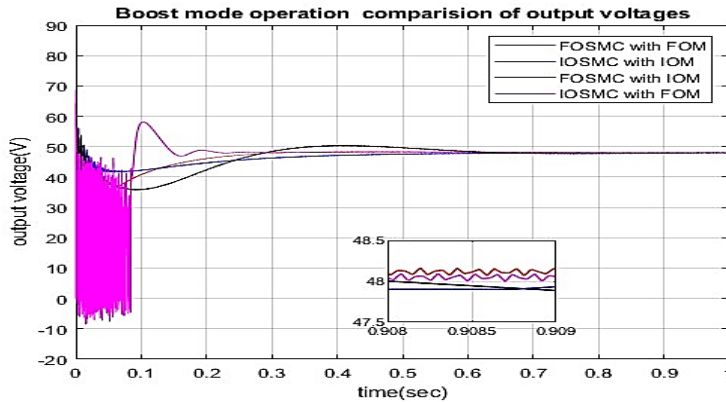


Figure 10. Comparison of Output Voltage for SEPIC and FOSEPIC Converters with FOSMC and IOSMC in Boost Mode Operation

Figure 10 presents a comparison of output voltage for both SEPIC and FOSEPIC converters under boost mode operation, highlighting the performance of different controllers. Panel (a) displays the results for the FOSMC with fractional order model (FOM) in [Red], while panel (b) shows the IOSMC with integer order model (IOM) in [Blue]. Panel (c) illustrates the FOSMC with IOM in [Black], and panel (d) depicts the IOSMC with FOM in [Magenta]. In both Figures 9 and 10, oscillations in the output voltage can be observed during the comparison between FOSMC and traditional SMC. The differentiation order is a critical factor, with integer orders used in IOM systems and fractional orders in FOM systems. This flexibility in fractional orders allows for richer dynamics and better tuning capabilities, making FOM an attractive option for control strategies.

Fractional-order control has emerged as a robust approach, effectively managing system uncertainties and disturbances while incorporating nonlinear dynamics. The combination of fractional-order control with SMC leads to the development of fractional-order sliding mode control (FOSMC), which improves upon traditional integer-order SMC.

#### **4. Conclusion**

This study successfully introduces a Fractional Order Sliding Mode Control (FOSMC) strategy with a simplified sliding surface function tailored for DC-DC FOSEPIC converters. By leveraging the input inductor current error, the proposed control method enables indirect regulation of output voltage, which significantly simplifies both the simulation process and the mathematical modeling involved. Extensive simulations conducted in MATLAB/SIMULINK under various operational conditions validate the performance of the FOSMC, showcasing its superior flexibility and enhanced control compared to traditional integer-order methods.

Additionally, this research pioneers the development of fractional-order models for SEPIC converters, offering a comprehensive framework that accurately captures their operational characteristics. The findings reveal that SEPIC converters equipped with fractional-order inductors and capacitors exhibit markedly improved dynamic performance, characterized by reduced overshoot and shorter regulation times when compared to conventional designs.

Overall, the integration of fractional-order control into sliding mode strategies not only enhances the robustness and performance of power conversion systems but also opens new avenues for future research and application. This innovative approach holds significant promise for advancing the efficiency and reliability of power electronics, particularly in the context of renewable energy systems and electric vehicle technologies. The results underscore the potential of fractional-order control as a key enabler for next-generation power management solutions, paving the way for more adaptive and high-performance systems in the field.

#### **Acknowledgment**

All the authors are contributed equally. The corresponding author is Dr Amruth Ramesh Thelkar, Assistant Professor G-III, Department of Electrical & Electronics Engineering, Nitte Meenakshi Institute of Technology, Bangalore, Karnataka, India, (An Autonomous Institution Affiliated to Visvesvaraya Technological University, Belagavi and approved by UGC), and Visiting Researcher, Faculty of Electrical & Computer Engineering, Jimma Institute of Technology, Jimma University, Ethiopia.

## Data Availability

The data used to support the findings of this study are available from the corresponding author upon request.

## Conflicts of Interest

The authors declare that they have no conflicts of interest

## References

- [1] B. Bandyopadhyay and S. Kamal, *Stabilization and control of fractional order systems: A sliding mode approach*, vol. 317. 2015. doi: 10.1007/978-3-319-08621-7\_1.
- [2] N. Yang, C. Wu, R. Jia, and C. Liu, "Fractional-Order Terminal Sliding-Mode Control for Buck DC/DC Converter," *Math. Probl. Eng.*, vol. 2016, 2016, doi: 10.1155/2016/6935081.
- [3] J. Zhou, "Nyquist-Like Stability Criteria for Fractional-Order Linear Dynamical Systems", *Control Theory in Engineering*, *IntechOpen*, doi: 10.5772/intechopen.88119.
- [4] H. Komijani, M. Masoumnezhad, M. M. Zanjireh, and M. Mir, "Robust Hybrid Fractional Order Proportional Derivative Sliding Mode Controller for Robot Manipulator Based on Extended Grey Wolf Optimizer," *Robotica*, pp. 1–12, 2019, doi: 10.1017/S0263574719000882.
- [5] R. Shalaby, M. El-Hossainy, and B. Abo-Zalam, "Fractional order modeling and control for under-actuated inverted pendulum," *Commun. Nonlinear Sci. Numer. Simul.*, vol. 74, pp. 97–121, 2019, doi: 10.1016/j.cnsns.2019.02.023.
- [6] A. Razminia and D. Baleanu, "Fractional order models of industrial pneumatic controllers," *Abstr. Appl. Anal.*, vol. 2014, 2014, doi: 10.1155/2014/871614.
- [7] H. Komurcugil, S. Biricik, and N. Guler, "Indirect Sliding Mode Control for DC-DC SEPIC Converters," *IEEE Trans. Ind. Informatics*, vol. 16, no. 6, pp. 4099–4108, 2020, doi: 10.1109/TII.2019.2960067.
- [8] S. Xu, G. Sun, Z. Ma, and X. Li, "Fractional-Order Fuzzy Sliding Mode Control for The Deployment of Tethered Satellite System under Input Saturation," *IEEE Trans. Aerosp. Electron. Syst.*, vol. PP, no. c, p. 1, 2018, doi: 10.1109/TAES.2018.2864767.
- [9] Y. Zhang and H. Li, "Adaptive Sliding Mode Control for SEPIC Converter," *Int. J. Electr. Power Energy Syst.*, vol. 144, p. 108947, 2023, doi: 10.1016/j.ijepes.2023.108947.
- [10] M. A. and A. Younis, "Nonlinear Control of SEPIC Converter for Photovoltaic Systems," *J. Power Electron.*, vol. 23, no. 4, pp. 789–800, 2023, doi: 10.1016/j.ijepes.2023.108947.
- [11] G. Liang and J. Hao, "Passive Synthesis of Immittance for Fractional-Order Three-Element-Kind Circuit," *IEEE Access*, vol. 7, pp. 58307–58313, 2019, doi: 10.1109/ACCESS.2019.2913911.
- [12] J. Liu, *Sliding mode control using MATLAB*. 2017.
- [13] A. A. Z. Diab, B. Ayalew, A. A. Yahaya, M. Debbouza, A. Al Durra, and A. Al Sumaiti, "Robust controller for grid-tied PV inverters based on continuous non-linear predictive and integral sliding mode control," *IET Power Electron.*, vol. 15, no. 15, pp. 1772–1784, 2022, doi: 10.1049/pel2.12344.
- [14] R. Ebrahimi, H. M. Kojabadi, L. Chang, and F. Blaabjerg, "Coupled-inductor-based high step-up DC-DC converter," *IET Power Electron.*, vol. 12, no. 12, pp. 3093–3104, 2019, doi: 10.1049/iet-pel.2018.6151.

- [15] J. Qiu and Y. Ji, "Observer-Based Robust Controller Design for Nonlinear Fractional-Order Uncertain Systems via LMI," *Math. Probl. Eng.*, vol. 2017, 2017, doi: 10.1155/2017/8217126.
- [16] L. Liu and S. Zhang, "Robust fractional-order PID controller tuning based on bode's optimal loop shaping," *Complexity*, vol. 2018, 2018, doi: 10.1155/2018/6570560.
- [17] X. Chen, Y. Chen, B. Zhang, and D. Qiu, "A Modeling and Analysis Method for Fractional-Order DC-DC Converters," *IEEE Trans. Power Electron.*, vol. 32, no. 9, pp. 7034–7044, 2017, doi: 10.1109/TPEL.2016.2628783.
- [18] J. Xu, X. Li, H. Liu, and X. Meng, "Fractional-Order Modeling and Analysis of a Three-Phase Voltage Source PWM Rectifier," *IEEE Access*, vol. 8, pp. 13507–13515, 2020, doi: 10.1109/ACCESS.2020.2965317.
- [19] P. Roy and B. K. Roy, "Sliding Mode Control Versus Fractional-Order Sliding Mode Control: Applied to a Magnetic Levitation System," *J. Control. Autom. Electr. Syst.*, vol. 31, no. 3, pp. 597–606, 2020, doi: 10.1007/s40313-020-00587-8.
- [20] Z. Jia and C. Liu, "Fractional-Order Modeling and Simulation of Magnetic Coupled Boost Converter," vol. 28, no. 5, pp. 1–15, 2018, doi: 10.1142/S021812741850061X.
- [21] S. Pashaei and M. A. Badamchizadeh, "Control of a class of fractional-order systems with mismatched disturbances via fractional-order sliding mode controller," *Trans. Inst. Meas. Control*, vol. 42, no. 13, pp. 2423–2439, 2020, doi: 10.1177/0142331220912070.
- [22] M. B. Delghavi, S. Shoja-Majidabad, and A. Yazdani, "Fractional-Order Sliding-Mode Control of Islanded Distributed Energy Resource Systems," *IEEE Trans. Sustain. Energy*, vol. 7, no. 4, pp. 1482–1491, 2016, doi: 10.1109/TSTE.2016.2564105.
- [23] L. Khoshnevisan and X. Liu, "Fractional order predictive sliding-mode control for a class of nonlinear input-delay systems: singular and non-singular approach," *Int. J. Syst. Sci.*, vol. 50, no. 5, pp. 1039–1051, 2019, doi: 10.1080/00207721.2019.1587030.
- [24] S. Kamal, R. K. Sharma, T. N. Dinh, M. S. Harikrishnan, and B. Bandyopadhyay, "Sliding mode control of uncertain fractional-order systems: A reaching phase free approach," *Asian J. Control*, vol. 23, no. 1, pp. 199–208, 2021, doi: 10.1002/asjc.2223.
- [25] S. Huang and J. Wang, "Fixed-time fractional-order sliding mode control for nonlinear power systems," *JVC/Journal Vib. Control*, vol. 26, no. 17–18, pp. 1425–1434, 2020, doi: 10.1177/1077546319898311.
- [26] S. Zhang, L. Liu, D. Xue, and Y. Q. Chen, "Stability and resonance analysis of a general non-commensurate elementary fractional-order system," *Fract. Calc. Appl. Anal.*, vol. 23, no. 1, pp. 183–210, 2020, doi: 10.1515/fca-2020-0007.
- [27] W. De J Kremes, P. J. S. Costa, C. H. I. Font, and T. B. Lazzarin, "Single-phase hybrid discontinuous conduction mode SEPIC rectifiers integrated with ladder-type switched-capacitor cells," *IET Power Electron.*, vol. 12, no. 11, pp. 2832–2842, 2019, doi: 10.1049/iet-pel.2019.0119.
- [28] J. Wang, C. Shao, and Y. Q. Chen, "Fractional order sliding mode control via disturbance observer for a class of fractional order systems with mismatched disturbance," *Mechatronics*, vol. 53, no. May, pp. 8–19, 2018, doi: 10.1016/j.mechatronics.2018.05.006.



- [29] T. Binazadeh and M. Yousefi, "Designing a Cascade-Control Structure Using Fractional-Order Controllers: Time-Delay Fractional-Order Proportional-Derivative Controller and Fractional-Order Sliding-Mode Controller," *J. Eng. Mech.*, vol. 143, no. 7, p. 4017037, 2017, doi: 10.1061/(asce)em.1943-7889.0001234.
- [30] O. Eray and S. Tokat, "The design of a fractional-order sliding mode controller with a time-varying sliding surface," *Trans. Inst. Meas. Control*, vol. 42, no. 16, pp. 3196–3215, 2020, doi: 10.1177/0142331220944626.
- [31] S. K. Damarla and M. Kundu, - *Fractional Order Processes: Simulation, Identification, and Control*. 2018. doi: 10.1201/9780429504433.
- [32] I. Petras, "Fractional Derivatives, Fractional Integrals, and Fractional Differential Equations in Matlab," *Eng. Educ. Res. Using MATLAB*, 2011, doi: 10.5772/19412.
- [33] R. Caponetto, G. Dongola, L. Fortuna, and I. Petras, *Fractional order systems. Modeling and control applications*, vol. Series A. 2010.